Astronomy & Astrophysics manuscript no. CBH
February 15, 2016

On recent SFR calibrations and the constant SFR approximation

M. Cerviño[1,2,3], A. Bongiovanni[1,2,4], and S. Hidalgo[1,2]

[1] Instituto de Astrofísica de Canarias, c/ vía Láctea s/n, 38205 La Laguna, Tenerife, Spain
[2] Departamento de Astrofísica, Universidad de La Laguna (ULL), 38205 La Laguna, Tenerife, Spain
[3] Instituto de Astrofísica de Andalucía (IAA-CSIC), Placeta de la Astronomía s/n, E-18008 Granada, Spain
[4] Asociación ASPID, Apartado de Correos 412, 38200 La Laguna, Tenerife, Spain

February 15, 2016

ABSTRACT

Aims. Star Formation Rate (SFR) inferences are based in the so-called constant SFR approximation, where synthesis models are require to provide a calibration; we aims to study the key points of such approximation to produce accurate SFR inferences.
Methods. We use the intrinsic algebra used in synthesis models, and we explore how SFR can be inferred from the integrated light without any assumption about the underling Star Formation history (SFH).
Results. We show that the constant SFR approximation is actually a simplified expression of more deeper characteristics of synthesis models: It is a characterization of the evolution of single stellar populations (SSPs), acting the SSPs as sensitivity curve over different measures of the SFH can be obtained. As results, we find that (1) the best age to calibrate SFR indices is the age of the observed system (i.e. about 13 Gyr for $z = 0$ systems); (2) constant SFR and steady-state luminosities are not requirements to calibrate the SFR; (3) it is not possible to define a SFR single time scale over which the recent SFH is averaged, and we suggest to use typical SFR indices (ionizing flux, UV fluxes) together with no typical ones (optical/IR fluxes) to correct the SFR from the contribution of the old component of the SFH, we show how to use galaxy colors to quote age ranges where the recent component of the SFH is stronger/softer than the older component.
Conclusions. Particular values of SFR calibrations are (almost) not affect by this work, but the meaning of what is obtained by SFR inferences does. In our framework, results as the correlation of SFR time scales with galaxy colors, or the sensitivity of different SFR indices to sort and long scale variations in the SFH, fit naturally. In addition, the present framework provides a theoretical guide-line to optimize the available information from data/numerical experiments to improve the accuracy of SFR inferences.

Key words. galaxies: star formation – galaxies: stellar content

1. Introduction

The knowledge of the amount of gas transformed into stars as a function of time, so called the star formation history, (SFH, $\psi(t)$), or at least the amount of gas transformed in stars recently (star formation rate, SFR, $\psi(\mathrm{t_{now}})$, or $\psi(t)$ averaged over a recent time inteval) is one of the key points to understand galaxy evolution and how and when the gaseous mass has been assembled into stars over cosmic times (see Madau & Dickinson 2014, for a recent review). The question about the *evolution of the gas and stars in galaxies* is a broad research area which is described in a formal way (evolutionary population synthesis models) in seminal papers as the one by B. Tinsley (1980). The formalism presented in the 80's had remained practically identical up to present days, being developments related with the use of observations to restrict the theoretical parameter space, or to use the models as a tool to infer physical parameters from observed quantities, as it is the case of SFR inferences.

The methodology used in recent SFH inferences is driven by observational trends of galaxy colors (see Kennicutt 1998), being evolutionary synthesis models used to calibrate the relation between a suitable observed integrated luminosity $\mathcal{L}_{\rm ind}$ and the recent SFH associated to such luminosity, $\mathcal{SFR}_{\rm ind}$.

Using the so-called constant SFR approximation (Kennicutt 1998), it is assumed a constant SFH up to an age $\mathrm{t_{test}}$, so suitable luminosities are these ones which reach a quasi steady-state value $\ell^{\rm asymp}_{\rm c\mathcal{SFR},ind}$ after some age $\mathrm{t_{ind}}$ lower than $\mathrm{t_{test}}$. Provided that the age $\mathrm{t_{ind}}$ is low enough, the term "recent" can be applied.

This situation can be described in general, independently of the final $\mathrm{t_{ind}}$ value, by the condition

$$\ell_{\rm c\mathcal{SFR},ind}(\mathrm{t_{ind}}) \simeq \ell_{\rm c\mathcal{SFR},ind}(t) \;\; \forall t \in [\mathrm{t_{ind}}, \mathrm{t_{test}}], \qquad (1)$$

although such mathematical refinement is usually not taken into consideration since an asymptotic behavior can we observed by a naked-eye inspection by plotting the time evolution of $\ell_{\rm c\mathcal{SFR},ind}(t)$ produced by the models, or by inspection of the numerical values given by the corresponding tables. As final result, the value $\ell_{\rm c\mathcal{SFR},ind}(\mathrm{t_{test}})$ is used as the asymptotic luminosity $\ell^{\rm asymp}_{\rm c\mathcal{SFR},ind}$, since, actually, $\mathrm{t_{ind}}$ is not required to be computed explicitly (in addition it avoids further complications about to give a quantitative meaning to the symbol "$\simeq$" used in Eq. 1; but see below).

Given that $\ell^{\rm asymp}_{\rm c\mathcal{SFR},ind}$ is obtained under a constant SFH assumption and normalized to a suitable SFR value (typically 1 $\mathrm{M_\odot/yr}$), we can obtain the associated SFR, $\mathrm{c}\mathcal{SFR}_{\rm ind}$, from the observed integrated luminosity $\mathcal{L}_{\rm ind}$ as,

$$\mathrm{c}\mathcal{SFR}_{\rm ind} = \mathcal{L}_{\rm ind} \times C_{\rm ind}, \qquad (2)$$

being

$$C_{\rm ind} = \frac{1}{\ell^{\rm asymp}_{\rm c\mathcal{SFR},ind}} = \frac{1}{\ell_{\rm c\mathcal{SFR},ind}(\mathrm{t_{test}})} \qquad (3)$$

Send offprint requests to: M. Cerviño, e-mail: mcs@iaa.es

In this methodology the main relevant parameter is t_{test}, which combines (1) our confidence that an asymptotic value had been actually reached at t_{test}, and (2) our believes about how a constant SFH is a valid approximation. As a reasonable compromise, t_{test} is chosen to conciliate both expectations, being a typical value t_{test} = 100Myr (e.g. Kennicutt 1998; Murphy et al. 2011). This choice of t_{test} can be justified as (a) the typical life-times of massive stars which produce each particular SFR proxy $\mathcal{L}_{ind}$, so we expect that $t_{test} \sim t_{ind}$, and (b) an age range large enough to include a large amount of burst-like star forming events formed at different ages (which at global level approaches to a constant SFH), so the obtained SFR represents an average of the SFH in the last t_{test} time interval. Implicitly is assumed that stars older that t_{test} almost do not contribute to $\mathcal{L}_{ind}$, and since population colors reders with age, it is expected that the bluer the galaxy the better the inference about the real SFR (Kennicutt 1998). The proposed calibration was originally establish for the disk component or irregular type galaxies, so implicitly a correction from bulge component of the galaxy (the old componet contribution) should be required; however, the calibration has been applied extensively to any kind of galaxy (e.g. galaxy surveys) where such decomposition is not possible.

Maybe the principal characteristic of this approach is that, besides its simplicity and intrinsic assumptions, it provides a reasonably good SFR inferences in more wider situations than the ones implicit in the formulation, including situations where the recent SFH is clearly not constant (e.g. Boquien et al. 2014, where graphical illustrative examples can be found). Even more, it looks surprising that, although any star, whatever its age and initial mass, emits in the whole wavelength range, the overall contribution of old stars in the system looks to have almost no impact in current proxies of the SFR except in the cases of low SFR, (see discussion about in Sect. 5.4 of Conroy 2013), or for SFR indices related with dust emission at infrared wavelengths (see discusion in Hirashita et al. 2003, as an example) So, although not perfect, the methodology includes the main (and principal) ingredients required to estimate a SFR, and, depending the proxy, it would refer to the instantaneous SFR ($\psi(t_{now})$) or the averaged SFH over a recent time interval.

Recent observational developments (in both sensitivity and spatial resolution) have lead to the requirement of improving calibrations, and a lot effort has been done in this direction covering different aspects of the problem (see Calzetti 2013; Kennicutt & Evans 2012; Madau & Dickinson 2014, as reviews in the subject). As examples about improvements of t_{test} let us mention Boquien et al. (2014), who propose to use t_{test} = 1 Gyr to produce more accurate results of C_{ind} for GALEX/FUV, NUV and SDSS/*u* indices due to the tiny, but non null, contribution to the integrated luminosities due to stars with ages between 100 Myr to 1 Gyr; or Johnson et al. (2013), who use t_{test} = 10 Gyr to better match the SFR properties of a sample of (primary) dwarf galaxies where the SFH had been obtained from CMD analysis. Related with it, there are the efforts to characterize the time-scale over the SFR is measured, as the use of a luminosity-weighted effective age (Buzzoni 2002b; Boquien et al. 2014), or to evaluate the accuracy of C_{ind} by computing explicitly characteristics time scales $t_{ind,x\%}$ where some percentage x of the integrated light is produced, and comparing it with similar time scales obtained from SFH inferred using different methodologies (as CDMs analysis or SED fitting); see discussions in Leroy et al. (2012), Hao et al. (2011); Calzetti (2013); Johnson et al. (2013) or Simones et al. (2014) as examples.

However, in most cases, the improvements of the calibration deals with the computation of evolutionary synthesis models using more or less sophisticated SFH to obtain the final (numerical) values and to compare them with the numerical values obtained under the constant SFR (and t_{test}) hypothesis; that is, the focus is placed in the variations of C_{ind} (or characteristics time scales) in different situations. And, afterwards, and despite variations due to fluctuations of the recent SFH at short time-scales (e.g. Otí-Floranes & Mas-Hesse 2010), the constant SFR approximation looks to be a quite good job (modulus the choice of t_{test}). So, In this work we ask ourselves the following questions: Is there any theoretical argument to define an optimal value of t_{test}? Is a constant SFR requirement fundamental for the calibration? If yes, why do the calibrations work even for SFHs that are raelly not constant?; if not, what is the physical meaning of the inferred value $c\mathcal{SFR}_{ind}$?

To answer such questions we require to understand how the SFH is implemented in synthesis codes in first instance; which is done in Sect.2. Secondly, we must understand what a synthesis code will provide independently of any specific choice of the SFH, and define the problem of SFR inferences using the algebra associated to synthesis models. To do so, we use first reasonable analytical approximations which provides hints and guidelines about different aspects of SFR calibrations/inferences (we recommend the woks of Tinsley 1980; Buzzoni 2002,b, 2005, which illustrates nicely this approach); before to compute the calibrations explicitly. This proccess is shown in Sect. 3. In Sect. 4 we apply the analysis about SFRs obtained in this work to corroborate and extend some results about SFR calibrations obtained recently. Our conclusions are presented in Sect. 5. In companion papers we will investigate the explicitly the sensitivity of SFR calibrations to the different choices of synthesis models (which results are briefly summarized in Sect. 3), and to how the overall SFH would affect (recent) SFR inferences. The overall idea developed in this paper implies to dismount some of the (unnecessary) assumptions about SFR inferences, so each section is written in schematic fashion.

2. SFH implementation in synthesis models

1. Evolutionary synthesis models are designed to describe the spectrophotometric evolution $\mathcal{L}_\lambda(t)$ of stellar ensembles (independently that other quantities are also obtained) for a given initial conditions. In our context, the initial conditions are some recipe providing how many stars of different initial masses had been formed at different time, (that is the stellar birth rate $\mathcal{B}(m,t)$), and the relation between luminosity at a given band/wavelength of an star given its initial mass and its evolutionary age t_*, $\ell_\lambda(m,t_*)$ [1].

2. Typically is assumed that $\mathcal{B}(m,t)$ can be decomposed in two independent functions, the one giving the frequency distribution of the initial masses of stars that would be formed whatever the age (it is, the initial mass function , IMF, $\phi(m)$) and other giving the the amount of stars formed at each time (it is, the star formation history, SFH, $\psi(t)$). The mass range where the stellar birth rate (hence the IMF) is defined must cover all physically posible stars formed $[m_{low}, m_{up}]$ and it is imposed by stellar physics. The time range where the stellar birth rate (hence the

[1] Actually it should read $\ell_\lambda(m,t_*,Z,\Omega)$, being Z the initial metallicity of the star, and Ω its rotational velocity, which implies to include the corresponding parameters in the stellar birth-rate. In addition, it can be also considered interactions between stars (i.e. binary interactions), which depend on additional parameters that, again, must be included in the stellar birth-rate. Along this work we neglect all such additional parameters.

SFH) is defined must include all the posible ages when a star of any mass would had been formed in the ensemble, so, in practical terms it covers from the time t_{ini} when the first star is formed in the observed system, to the (rest-frame) time where the observation is done t_{now}. In the case of galaxies and stellar ensembles inside galaxies, the value of t_{ini} is given by cosmological studies as far as we accept that there is an epoch of galaxy formation, and that any stellar ensemble inside a galaxy would contain a relic contribution of the first formed stars (a quite plausible assumption which depends on the movements/redistribution of stars formed at different times due to galactic dynamics). Finally, the value of t_{now} is imposed by the observation the redshift of the source and the choice of a cosmological model.

Being $\mathcal{B}(m,t)$ defined only in a time interval, we can define the age of the ensemble as the time interval since the first star has been formed up to the rest-frame present time, i.e. $t_{age} = t_{now} - t_{ini}$, encoding in it all the cosmological considerations; so $\mathcal{B}(m,t)$ is defined as $[0, t_{age}]$ being t the proper age of the global system. Assuming that both $\mathcal{B}(m,t)$ and $\ell_\lambda(m,t_*)$ are well comported and integrable functions, and taking into account that a star born at a time t has an estellar age $t_* = t_{age} - t$, the resulting luminosity of the ensemble $\mathcal{L}_\lambda(t_{age})$ at any t_{age} value is obtained as:

$$\begin{aligned}\mathcal{L}_\lambda(t_{age}) &= \int_0^{t_{age}} \int_{m_{low}}^{m_{up}} \ell_\lambda(m, t_{age}-t)\,\mathcal{B}(m,t)\;\mathrm{d}m\,\mathrm{d}t \\ &= \int_0^{t_{age}} \left[\int_{m_{low}}^{m_{up}} \ell_\lambda(m, t_{age}-t)\,\phi(m)\mathrm{d}m\right]\psi(t)\,\mathrm{d}t \\ &= \int_0^{t_{age}} \ell_{\lambda,\mathrm{IMF}}(t_{age}-t)\,\psi(t)\,\mathrm{d}t \end{aligned} \quad (4)$$

where the term $\ell_{\lambda,\mathrm{IMF}}(t_{age}-t) = \ell_{\lambda,\mathrm{IMF}}(t_*)$ refers to the integrated luminosity when only stars with the same stellar age t_* are considered. Since such situation can be also described as the resulting luminosity when the SFH is described as a Dirac's delta distribution, this quantity is usually referred as the integrated luminosity of a single age (single metallicity) stellar population, or SSP. Although we use the term SSP along the work, since commonly used in the literature, we keep the notation $\ell_{\lambda,\mathrm{IMF}}(t_*)$, which explicitly shows that such result actually does not include information about the SFH, neither it represents an integrated luminosity but just an useful mathematical entity which only contains information about the stellar evolution (and $\phi(m)$), which is always well defined.

3. A simple inspection of Eq. 4 shows that $\mathcal{L}_\lambda(t_{age})$, which is the only observable quantity, is always evaluated over the complete age range where the SFH $\psi(t)$ and the SSP luminosities $\ell_{\lambda,\mathrm{IMF}}(t_*)$ are defined. Any stellar population synthesis computation including all stellar evolutionary phases shows that $\ell_{\lambda,\mathrm{IMF}}(t_*)$ never reach a zero value, so

> the most plausible t_{test} to be used to calibrate recent SFR indices is the age of the system t_{age} (which has a value around 13 Gyr in the local Universe), since it is the intrinsic time provided by the observable luminosity.

We cannot escape from this result: Whatever the observable luminosity, it includes the contribution of stars covering all possible range of stellar ages t_* from 0 (just born stars at t_{now}) to t_{age} (the first formed stars in the system that are still alive). There is no way to discriminate the contribution of stars with different ages without knowing the whole SFH, or equivalently, we cannot calibrate a SFR by constraint the SFH to our concept of "recent" encoded in a t_{test} value. The result would be shocking for some readers, since following literally the methodology to calibrate the SFR, it would imply to assume a constant SFH all over the life-time of the galaxy; a result that hardly conciliates with our current understanding of galaxy evolution. And ever more shocking taking into account that the calibrations used in the literature, although assume a t_{test} much lower than t_{age}, produce in average a quite good job.

4. The solution to such apparent muddle is to change the perspective about the role of the SFH in the calibration of SFR indices: the approximation used to calibrate SFR indices does not deal with any particular SFH, but with $\ell_{\lambda,\mathrm{IMF}}(t_*)$; a constant SFH assumption is equivalent to use no information at all about the SFH. Would be $\mathcal{L}_\lambda(t_{age})$ produced by, and only by, stars with ages t_* equal or lower than t_{ind}, then, whatever the functional form of $\psi(t)$, the associated integrated luminosity is the result of the SFH restricted to the time interval $[t_{now} - t_{ind}, t_{now}]$. Even more, such $\mathcal{L}_\lambda(t_{age})$ reach a steady state for any $t_{age} > t_{ind}$, and a $\ell_{\lambda,\mathrm{IMF}}(t_*)$-weighted averaged SFH over the last t_{ind} age range (i.e. an SFR) can be obtained. So, although under such conditions, we can translate the situation to consider the SFH only defined up to t_{ind} and we will obtain the same result, it is the characteristics of the chosen luminosity (i.e. of $\ell_{\lambda,\mathrm{IMF}}(t_*)$) what allows to obtain SFR inferences, not the choice of any particular SFH. As result, the SFR calibration is actually a characterization of the evolution of SSP, $\ell_{\lambda,\mathrm{IMF}}(t_*)$, instead a question about the choice of a t_{test} value and $\psi(t)$ functional forms typically addressed in the literature. Let us exploit this idea in the following section.

3. The SFR calibration as a characterization of the evolution of SSP luminosity, $\ell_{\lambda,\mathrm{IMF}}(t_*)$, instead a constant SFR hypothesis

To fully exploit the statement and implications quoted in the previous section it is required a step by step process. In the following, let us use Eq. 4 with different (hypothetical and realistic) $\ell_{\lambda,\mathrm{IMF}}(t_*)$ functional forms to obtain results about SFR inferences. We stress that all along this section no hypothesis about the SFH is required.

3.1. SSP luminosity evolving as a hat function

1. As a first simple example, let us assume that the SSP luminosity $\ell_{\lambda,\mathrm{IMF}}(t_*)$ evolves as is a hat-function with a constant value $\ell_{\lambda,\mathrm{cte}}$ in a given time range $[t_{*,\mathrm{begin}}, t_{*,\mathrm{end}}]$, hence covering a time interval $\Delta t = t_{*,\mathrm{end}} - t_{*,\mathrm{begin}}$, and zero otherwise. Trivially Eq. 4 is only defined in the time interval $[t_{age} - t_{*,\mathrm{end}}, t_{age} - t_{*,\mathrm{begin}}]$ and, after some trivial operations,

$$\langle \mathcal{SFR} \rangle_{t_{*,\mathrm{end}},\Delta t} = \frac{\int_{t_{age}-t_{*,\mathrm{end}}}^{t_{age}-t_{*,\mathrm{begin}}} \psi(t)\mathrm{d}t}{\Delta t} = \frac{\mathcal{L}_\lambda(t_{age})}{\ell_{\lambda,\mathrm{cte}} \times \Delta t}, \quad (5)$$

where $\langle \mathcal{SFR} \rangle_{t_{*,\mathrm{end}},\Delta t}$ is exactly the mean value of the SFH in the corresponding time interval where $\ell_{\lambda,\mathrm{IMF}}(t_*)$ is defined. Note that, in order to understand such measure, two quantities are required: the associated time interval and one of the time boundaries. Trivially, if $t_{*,\mathrm{begin}} = 0$, we have $\Delta t = t_{*,\mathrm{end}}$ and only one parameter is needed. Let us denote such situation by maning $t_{*,\mathrm{end}}$ as $t_{*,\mathrm{ind}}$ and $\langle \mathcal{SFR} \rangle_{t_{*,\mathrm{end}},\Delta t}$ as $\langle \mathcal{SFR} \rangle_{\Delta t}$. In this situation, $\langle \mathcal{SFR} \rangle_{\Delta t}$ is an exact measure of the mean recent SFR in the last $\Delta t = t_{*,\mathrm{ind}}$ time range.

This measure of the SFR is completely independent of the details of the SFH functional form, working even for the case

of a burst of star formation where $\psi(t)$ is described as a Dirac's delta function with intensity $\mathcal{M}$: If such event happens in the quoted time interval, then $\mathcal{L}_\lambda(\mathrm{t_{age}}) = \mathcal{M} \times \ell_{\lambda,\mathrm{cte}}$, and the mean value of $\psi(t)$ in such time interval is $\mathcal{M}/\Delta t$.

2. Although a hat-function would be seen as an unrealistic case, this kind of distribution is similar to the description of how recent SFR is inferred from Young Stellar Objects (YSO) number counts N_{YSO}, which is typically used to introduce SFR inferences (e.g. Calzetti 2013; Kennicutt & Evans 2012). In that case it is only required a time scale τ_{YSO} where a YSO would be observed (which is given by the physics of star formation, which has a value around 2 Myr; see McKee & Ostriker 2007 or Evans et al. 2009 as examples). So the SFR inferred from the observation of N_{YSO} YSO in units of number of stars formed by unit time is:

$$\langle \mathcal{SFR} \rangle_{\tau_{\mathrm{YSO}}} = \frac{N_{\mathrm{YSO}}}{\tau_{\mathrm{YSO}}}, \tag{6}$$

Implicitly we are neglecting the information that the luminosity of each YSO would provide about when such object is formed, which is equivalent to assume *de facto* that a hat function defined in the time interval $[0, \tau_{\mathrm{YSO}}]$. Hence, independently of posible variations of $\psi(t)$ in such time interval, a correct average $\langle \mathcal{SFR} \rangle_{\tau_{\mathrm{YSO}}}$ is obtained[2].

3. Although we know that no SSP luminosity $\ell_{\lambda,\mathrm{IMF}}(t_*)$ evolves as a hat function, the hat function case shows that we cannot obtain $\psi(\mathrm{t_{now}})$ from observations, but, at best, an average value over a time interval $\langle \mathcal{SFR} \rangle_{\Delta t}$. We can extend the concept of average the SFR over a time interval, to the concept of obtain a weighted mean of $\psi(t)$ over any arbitrary function $\varphi_\lambda(t)$. The only requirement is that such function is normalized over the time interval $\psi(t)$ is defined (i.e. $\mathrm{t_{age}}$). In the context of this paper, we can define the weight function $\varphi_\lambda(t)$ as:

$$\varphi_\lambda(t) = \frac{\ell_{\lambda,\mathrm{IMF}}(\mathrm{t_{age}} - t)}{\int_0^{\mathrm{t_{age}}} \ell_{\lambda,\mathrm{IMF}}(\mathrm{t_{age}} - t)\, \mathrm{d}t} = \frac{\ell_{\lambda,\mathrm{IMF}}(\mathrm{t_{age}} - t)}{\int_0^{\mathrm{t_{age}}} \ell_{\lambda,\mathrm{IMF}}(t_*)\, \mathrm{d}t_*}. \tag{7}$$

So the SFH $\varphi_\lambda(t)$-weighted mean, $\langle \mathcal{SFR} \rangle_\lambda$, is:

$$\begin{aligned} \langle \mathcal{SFR} \rangle_\lambda &= \int_0^{\mathrm{t_{age}}} \psi(t)\, \varphi_\lambda(t) dt = \\ &= \frac{\int_0^{\mathrm{t_{age}}} \psi(t)\, \ell_{\lambda,\mathrm{IMF}}(\mathrm{t_{age}} - t)\, \mathrm{d}t}{\int_0^{\mathrm{t_{age}}} \ell_{\lambda,\mathrm{IMF}}(t_*)\, \mathrm{d}t_*} \\ &= \frac{\mathcal{L}_\lambda(\mathrm{t_{age}})}{\int_0^{\mathrm{t_{age}}} \ell_{\lambda,\mathrm{IMF}}(t_*)\, \mathrm{d}t_*} = C_\lambda \times \mathcal{L}_\lambda(\mathrm{t_{age}}). \end{aligned} \tag{8}$$

The normalization coefficient of the function $\varphi_\lambda(t)$ is the inverse of the quantity $C_\lambda \equiv C_{\mathrm{ind}}$ used in the usual calibrations of the SFR. Of course, such normalization coefficient can be also interpreted as the luminosity obtained by a synthesis model under a constant SFH assumption, but actually

> a constant SFR assumption is not a requirement to calibrate SFR indices. It is the evolution of the SSP luminosity (the $\ell_{\lambda,\mathrm{IMF}}(t_*)$ function) normalized over the system age, not a hypothesis about the SFH $\psi(t)$, which gives the meaning to the $\langle \mathcal{SFR} \rangle_\lambda$ that can be obtained from observations.

An alternative interpretation to Eq. 8 is that the observed luminosity $\mathcal{L}_\lambda(\mathrm{t_{age}})$ is the result of the SFH $\psi(t)$ once filtered over the evolution of the luminosity produced by coeval stars $\ell_{\lambda,\mathrm{IMF}}(t_*)$ (defined up to $t_* = \mathrm{t_{age}}$). So, we can obtain direct information about $\psi(t)$ once the filter is normalized/calibrated, or, in general grounds, when the zero point of the filter is defined in a similar way that in photometric studies[3].

4. Previous result is general, so, if we hope that $\langle \mathcal{SFR} \rangle_\lambda$ contains only information about the recent SFH, we require a filter only sensitive to recent ages. That is, an hypothetical $\mathcal{L}_\lambda(\mathrm{t_{age}})$ which associated $\ell_{\lambda,\mathrm{IMF}}(t_*)$ has a zero value after some age $t_{*,\mathrm{ind}}$. Such break, if exists, can be obtained by a direct inspection of $\ell_{\lambda,\mathrm{IMF}}(t_*)$, but also by the variation over t_* of the integral of $\ell_{\lambda,\mathrm{IMF}}(t_*)$. Trivially, if it goes to zero after at some $t_{*,\mathrm{ind}}$ value, then

$$\int_0^{\mathrm{t_{age}}} \ell_{\lambda,\mathrm{IMF}}(t_*)\mathrm{d}t_* \equiv \int_0^{\mathrm{t_{*,ind}}} \ell_{\lambda,\mathrm{IMF}}(t_*)\mathrm{d}t_* \equiv \ell^{\mathrm{asymp}}_{\lambda,\mathrm{c}\mathcal{SFR}} \;\; \forall t > t_{*,\mathrm{ind}},$$

being $\ell^{\mathrm{asymp}}_{\lambda,\mathrm{c}\mathcal{SFR}} = \ell_{\lambda,\mathrm{cte}} \times \Delta t$ for the case of a hat function. We have keep the symbol $\ell^{\mathrm{asymp}}_{\lambda,\mathrm{c}\mathcal{SFR}}$ to stress its similitude with the calibration constant C_{ind} (Eqs. 3, 5, 8).

5. The use of the integral over t_* instead a direct inspection of $\ell_{\lambda,\mathrm{IMF}}(t_*)$ would be seen as an unnecessary complication. However, the $\ell_{\lambda,\mathrm{IMF}}(t_*)$ obtained by synthesis codes (or equivalently, the evolution of SSP models) are not hat-like functions, neither shows a clear well defined $t_{*,\mathrm{ind}}$ value. Rather than that, shows that the luminosity declines with t_* more or less quickly depending on the wavelength. So, if we still aims to obtain a $\langle \mathcal{SFR} \rangle_\lambda$ value which can be used as the actual $\langle \mathcal{SFR} \rangle_{\Delta t}$ for some observed $\mathcal{L}_\lambda(\mathrm{t_{age}})$ luminosity, the look for $\ell_{\lambda,\mathrm{IMF}}(t_*)$ whose integral over time reach a quasi-state regime is the only approach, being $\Delta t (\equiv \mathrm{t_{ind}})$ defined by the age where such steady-state is reached.

3.2. SSP luminosity evolving as a hat function plus a power law decay

1. Going forward, let us use a second still simplified but more realistic functional form of the SSP luminosity evolution. Assuming a properly defined zero age main sequence, all stars increasing its luminosity (at least in UV to IR wavelengths) up to the end of the main sequence; hence any $\ell_{\lambda,\mathrm{IMF}}(t_*)$ will have a first period with a slow increase of its luminosity at least up to the age $\mathrm{t_{*,MS}}$ where more massive stars leave the main sequence, which is typically 3 Myr. After that age, the presence of post-main sequence evolutionary phases result in a more complicate evolution. However, simple energetic arguments show that, in a quite reasonable approximation, $\ell_{\lambda,\mathrm{IMF}}(t_*)$ evolves as a declining power law. It is a classical result (Tinsley & Gunn 1976; Buzzoni 1995) still confirmed by comparisons with current synthesis models and proven as an useful approximation (Buzzoni 2005). Just for simplicity, let us assume that $\ell_{\lambda,\mathrm{IMF}}(t_*)$ is constant

[2] Actually the time dependence of the luminosity is used in works dealing with the star formation process itself where different classes of YSO are considered; see Lada et al. (2013); Román-Zúñiga et al. (2015) as examples.

[3] The analogy of synthesis models results and photometry is not new and it is quoted by Shore (2002) Chap. 7, Sect. 3.3; surprising such analogy has been poorly explored in the literature, and typically limited to restricted $\mathrm{t_{test}}$ values; however, see Otí-Floranes & Mas-Hesse (2010); Leroy et al. (2012) as counterexamples who, the facto, use $\ell_{\lambda,\mathrm{IMF}}(t)$ as SFH-sensitivity curve.

index	α	$\langle t_*\rangle_\lambda$ 10^6 yr	% at $\langle t_*\rangle_\lambda$	$t_{\lambda,99\%}$ 10^6 yr	$t_{\lambda,95\%}$ 10^6 yr	$t_{\lambda,90\%}$ 10^6 yr	$t_{\lambda,80\%}$ 10^6 yr	$t_{\lambda,50\%}$ 10^6 yr
generic $Q(H)$	> 2.00	< 13	>89%	<148	< 30	< 15	< 7.5	< 3
generic UV	1.50	131	91%	3325	375	112	31	5
generic U	1.10	937	80%	11156	6187	3100	885	43
generic IR/V	0.80	2549	67%	12457	10462	8337	5120	817
α values from comparison with synthesis models in Sect. 3.3								
$Q(H)$	4.00	2	56%	9	5	4	3	2
GALEX/FUV	1.55	101	91%	2386	254	80	24	5
GALEX/NUV	1.50	131	91%	3325	375	112	31	5
SDSS/u	1.07	1060	79%	11401	6824	3683	1156	58
SDSS/g	0.88	2055	71%	12284	9753	7243	3861	413
SDSS/r	0.75	2865	65%	12534	10796	8885	5834	1157
SDSS/i	0.72	3055	64%	12573	10965	9170	6228	1388
SDSS/z	0.66	3430	62%	12636	11246	9656	6936	1890

Table 1. Values of the slope of the SSP luminosity evolution $\ell_{\lambda,\mathrm{IMF}}(t_*)$ when modeled as a power law α (see below), the mean age of $\ell_{\lambda,\mathrm{IMF}}(t_*)$ denoted as $\langle t_*\rangle_\lambda$, the percentage of the sensitivity of $\ell_{\lambda,\mathrm{IMF}}(t_*)$ in the 0 to $\langle t_*\rangle_\lambda$ age range, and the ages where the sensitivity to $\ell_{\lambda,\mathrm{IMF}}(t_*)$ reach a x% value of the total sensitivity, $t_{\lambda,x\%}$, for 99, 95, 90, 80 and 50% for the set of bands used in this work. The results assume that $\ell_{\lambda,\mathrm{IMF}}(t_*)$ is flat up to 3 Myr and follows a decreasing power law with exponent α for larger ages up to t_{age} = 13 Gyr. The upper part of the table shows the generic α values used in this section for different bands guided by the results in Fig. 1. The lower part of the table shows α values chosen a posteriori to roughly fit the results of detailed computations presented in Sect. 3.3 (table 2).

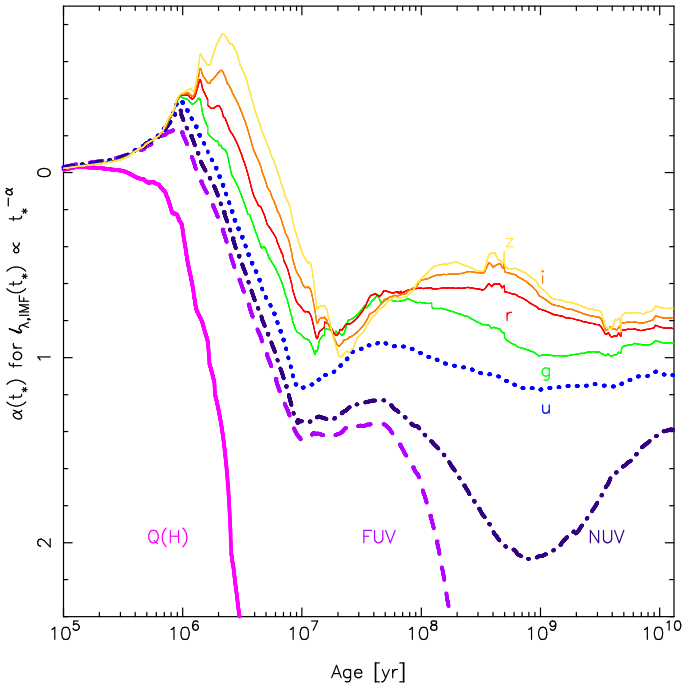

Fig. 1. Evolution of the slope of the approximation of SSP luminosity following power law evolution $\ell_{\lambda,\mathrm{IMF}}(t_*) \propto t_*^{-\alpha}$ (actually $\alpha(t_*)$) for different photometric bands obtained by the combination of different synthesis models (see Sect. 3.3 for details). The slope evolution of $Q(H)$ is only show up to 50 Myr and GALEX/FUV up to 200 Myr; in addition the slopes have been smoothed to represent the general aspect of the evolution. Note the non-standard orientation of the y-axis since refers to α values, whereas the slope is $-\alpha$.

in the interval $[0, t_{*,\mathrm{MS}}]$ and it evolves as $t_*^{-\alpha}$, from $t_{*,\mathrm{MS}}$ up to any posible t_{age}, being $\ell_{\lambda,\mathrm{MS}}$ the luminosity at $t_{*,\mathrm{MS}}$, so the evolution of such SSP luminosity is:

$$\ell_{\lambda,\mathrm{IMF}}(t_*) = \begin{cases} \ell_{\lambda,\mathrm{MS}} & \text{for } t_* \le t_{*,\mathrm{MS}}, \\ \ell_{\lambda,\mathrm{MS}} \left(\frac{t_*}{t_{*,\mathrm{MS}}}\right)^{-\alpha} & \text{for } t_* > t_{*,\mathrm{MS}}. \end{cases} \quad (9)$$

As reference values, α is around or lower than 1 for wavelengths larger than 3000Å (Buzzoni 2002). Table 1 in Buzzoni (2005) provides a detailed analysis including metallicity effects showing that the slope flattens when metallicity decreases. Also as reference, we show the evolution of α for different photometric bands obtained by the combination of different synthesis models (see Sect. 3.3 for details) in Fig. 1. In practical terms we will consider in this section generic values of α = 0.6 to 0.9 as representation of IR/visible bands, and α = 1.1, 1.5 and larger than 2 as generic representation of U band, UV bands, and the number of Hydrogen ionizing photons, ($Q(H)$, which is proportional to the emission luminosity of Hydrogen recombination lines, as the Hα emission line), respectively. The numerical results obtained here assumes $t_{*,\mathrm{MS}}$ = 3 Myr, and, when required, t_{age} = 13 Gyr. We show in Tab. 1 a more detailed version of specific values of α for different generic bands, and related quantities computed using the present approximation and discussed in this section. The lower part of the table shows α values chosen a posteriori to roughly fit the results when realistic synthesis models are used (Sec. 3.3, table 2). Note that for $Q(H)$ we use here a generic value of $\alpha > 2$ as a limit although a value of $\alpha = 4$ would be more realistic nominal value.

2. The integral over time of such $\ell_{\lambda,\mathrm{IMF}}(t_*)$ for $t > t_{*,\mathrm{MS}}$ can be obtained analytically:

$$\int_0^t \ell_{\lambda,\mathrm{IMF}}(t_*)\mathrm{d}t_* = \begin{cases} \frac{\ell_{\lambda,\mathrm{MS}}\, t_{\mathrm{MS}}}{\alpha-1}\left(\alpha - \left(\frac{t}{t_{\mathrm{MS}}}\right)^{1-\alpha}\right) & \text{for } \alpha \neq 1, \\ \ell_{\lambda,\mathrm{MS}}\, t_{\mathrm{MS}}\left(1 + \ln\frac{t}{t_{\mathrm{MS}}}\right) & \text{for } \alpha = 1. \end{cases} \quad (10)$$

Such integral only has an asymptote if $\alpha > 1$ with a value:

$$\ell_\lambda^{\mathrm{asymp}} = \frac{\ell_{\lambda,\mathrm{MS}}\, t_{\mathrm{MS}}\, \alpha}{\alpha - 1}. \quad (11)$$

So, the luminosity at wavelengths/bands larger than 3000Å never reach an asymptotical value and the sensitivity of the SSP evolution o the old SFH increases as the system evolves. This situation, when translated to the statement that the the time integral of the SSP luminosity reach an asymptotic value to define a reliable SFR index situates U in a limiting situation due to its metallicity dependence (Buzzoni 2005). Actually U is considered as a reliable index by some authors (e.j. Wilkins et al. 2012; Boquien et al. 2014, but see below) but not by others.

3. A direct comparison of Eqs. 10 and 11, allows to evaluate the difference between the real asymptotic value and the value obtained for any chosen t provided that $\alpha > 1$; hence to estimate possible values of t_{test} where an asymptotical values have been actually reached. Evaluating Eq. 10 at $t_* = 13$Gyr (1 Gyr, 100 Myr), and comparing with the asymptotic value we found that the asymptotic values is underestimated by 39% (51%, 64%) for $\alpha = 1.1$ corresponding to a generic U band; in the case of $\alpha = 1.5$ corresponging to FUV bands, the underestimate is 1% (4%, 12%). Finally the underestimation is less than 1 .5% in the three ages for $\alpha \geq 2$. So, with exception of Q(H) based indices (and neglecting their flattering at older ages, see sect. 3.3 below), asymptotical values are never reached given the age of the Universe! It is,

> to reach a steady state/quasi-asymptotic value, although desirable, cannot be a strong requirement to define and calibrate SFR indices since such asymptotic value is not reached even at cosmological time scales; actually the more close we would be to the asymptotic value is to use the one defined by the age of the system t_{age}.

Actually, a graphical inspection of the $C_{ind}(t_{test})$ values quoted in appendix of Boquien et al. 2014 shows that, excluding $Q(H)$ and apparently C_{FUV} at some metallicities, an asymptotical value of $C_{ind}(t_{test})$ at $t_{test} = 1$Gyr has been not reached.

4. The fact that asymptotic values can not be reached implies that we cannot define a characteristic time scale Δt which allows a direct transformation of $\langle \mathcal{SFR} \rangle_\lambda$ in $\langle \mathcal{SFR} \rangle_{\Delta t}$. We stress that it is implicit in the filter Nature gives us to infer the SFR (it is the power law nature of the evolution of SSP luminosities). However we can try to obtain some usable summaries of $\ell_{\lambda,\mathrm{IMF}}(t_*)$, which allows to obtain information without take into account the functional form of $\ell_{\lambda,\mathrm{IMF}}(t_*)$ explicitly; a similar problem related with the characterization of photometric systems, or probability distributions. A typical characterization is obtained by the computing of cumulative distributions of the amount of flux comprised from 0 up to a given t_* value (examples are the way SFR is calibrated; see also Leroy et al. 2012 or Johnson et al. 2013). In the following we show two alternative approaches used in the literature.

4.1. The first one is to define a *mean* luminosity-weighted age (Buzzoni 2002b; Boquien et al. 2014), which can we defined taking into account an assumed SFH;

$$\langle t_* \rangle_{\lambda,\psi(t)} = \frac{\int_0^{t_{age}} t_* \, \ell_{\lambda,\mathrm{IMF}}(t_*) \, \psi(t_{age} - t_*) \, \mathrm{d}t_*}{\int_0^{t_{age}} \ell_{\lambda,\mathrm{IMF}}(t_*) \, \psi(t_{age} - t_*) \, \mathrm{d}t_*}. \quad (12)$$

It can be used as a measure of the mean age of the stars which contributes to $\mathcal{L}_\lambda$ at different wavelengths, SFH and IMF slopes (e.g. Buzzoni 2002b).

Alternatively, it can be defined a characteristic weighted age of $\ell_{\lambda,\mathrm{IMF}}(t_*)$ without considerations about the SFH (or, equivalently at mathematical level, by assuming a constant SFH over all the galaxy life-time),

$$\langle t_* \rangle_\lambda = \frac{\int_0^{t_{age}} t_* \, \ell_{\lambda,\mathrm{IMF}}(t_*) \mathrm{d}t_*}{\int_0^{t_{age}} \ell_{\lambda,\mathrm{IMF}}(t_*) \mathrm{d}t_*}, \quad (13)$$

also used by Buzzoni (2002b), and Leroy et al. (2012) to study the sensitivity of SFR to recent SFH variations, or by Boquien et al. (2014) to investigate, by comparison with $\langle t_* \rangle_{\lambda,\psi(t)}$ the stability of $C_{ind}(t_{test})$ as a function of t_{test} and different SFHs. Using our power law approximation, $\langle t_* \rangle_\lambda$ can be obtained analytically using Eq.10 easily, having values of 2.5 Gyr (937, 131, 13 Myr) for $\alpha = 0.8$ (1.1, 1.5, 2). Such values are roughly in agreement with our expectations about Δt based in the stellar life-times which mainly contributes to different wavelengths.

The use of a simplified $\ell_{\lambda,\mathrm{IMF}}(t_*)$ also allows to compute easily the amount of sensitivity up to $\langle t_* \rangle_\lambda$, being the results shown in Table 1. Using first principles, given the L-shape nature of $\ell_{\lambda,\mathrm{IMF}}(t_*)$, we can assure that at least 50% of the sensitivity to the SFH is concentrated at ages equal or lower than $\langle t_* \rangle_\lambda$ for any band (including optical ones), although the value depends on α being a maximum value reached at $\alpha \sim 1.67$. So, as a remark, $\langle t_* \rangle_\lambda$ it provides valuable information, but it does not provide neither a cut-off in $\ell_{\lambda,\mathrm{IMF}}(t_*)$, nor a characteristic time over the recent SFH is averaged.

4.2. A second characterization of the evolution of SSP luminosities is to compute the ages $t_{\lambda,x\%}$ where the sensitivity of $\ell_{\lambda,\mathrm{IMF}}(t_*)$ to any SFH comprises x% of the total sensitivity, which is obtained solving:

$$\int_0^{t_{\lambda,x\%}} \ell_{\lambda,\mathrm{IMF}}(t_*)\mathrm{d}t_* = \frac{x}{100} \int_0^{t_{age}} \ell_{\lambda,\mathrm{IMF}}(t_*)\mathrm{d}t_*, \quad (14)$$

An advantage of $t_{\lambda,x\%}$ is that provide a more quantitative information that $\langle t_* \rangle_\lambda$. Again, it cannot be taken as a face-on value of Δt but, at least, provide information about how much of the sensitivity of the curve would be affected by the old component of the SFH.

Using our simplified evolution of SSP luminosities, we obtain values of $t_{\lambda,80\%}$ ($t_{\lambda,95\%}$) of 5.1 Gyr (10.5 Gyr) for $\alpha = 0.8$ which are SDSS/g filters; 885 Myr (6.2 Gyr) for $\alpha = 1.1$ or U band; 31 Myr (375 Myr) for $\alpha = 1.5$ or UV filters, and 7.5 Myr (30 Myr) for $\alpha = 2$, i.e. the ionizing flux (c.f, Tab 1). Values obtained using detailed synthesis models results are shown in Tab. 2 and discused in Sec. 3.3. Note that, given that $t_{\lambda,100\%} = t_{age}$ by construction, each $t_{\lambda,x\%}$ is also a measure about how far/close we are to the physical limiting value when $t_{\lambda,x\%}$ is used to define C_{ind}. Of course, as in the case of $\langle t_* \rangle_{\lambda,\psi(t)}$, the definition can be extended to any SFH (see Johnson et al. 2013, as an example).

5. As a summary of results, we have seen how our expectations about SFR inferences had been downgraded: we have first relaxed out expectations of obtain $\psi(t_{now})$ to obtain an averaged over a defined Δt, $\langle \mathcal{SFR} \rangle_{\Delta t}$. But given the nature of the integrated luminosity, we have downgrade again to obtain a $\langle \mathcal{SFR} \rangle_\lambda$ where a single time scale over the SFR has been averaged can no properly defined. The most we can obtain is the sensitivity of the given luminosity to the recent and old components of the global SFH. As a collateral result is that such kind of information can be obtained for any luminosity (not only the standard ones used a SFH indices). When applied to optical fluxes, we obtain that 50% of the sensitivity of the integrated luminosity is concentrated at ages lower than 2 Gyr, so such wavelengths still contains a valuable information about the recent (lower than 2 Gyr) SFH of the system. Such wavelengths can be used to constraint the quality of SFR inferences obtained by bona fide indices as we will se below.

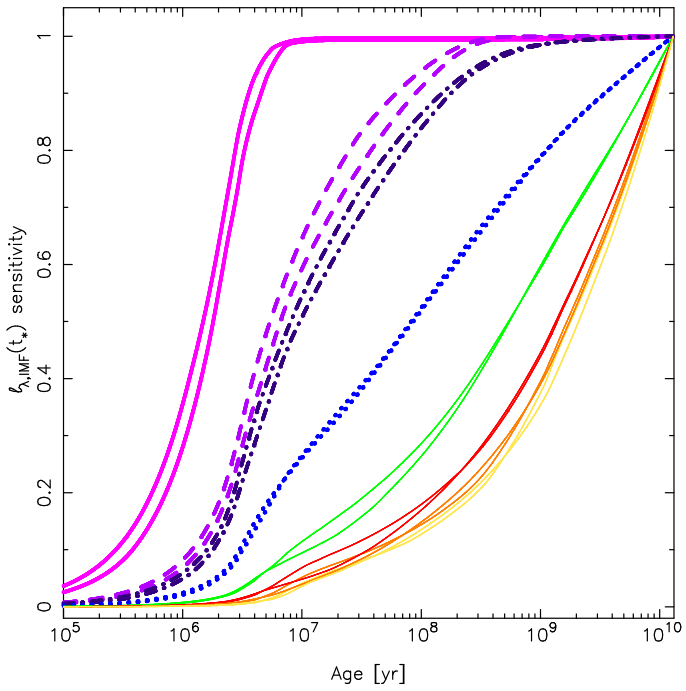

Fig. 2. Evolution of the sensitivity of the SSP luminosity $\ell_{\lambda,\mathrm{IMF}}(t_*)$ with the age using the upper and lower envelopes of SSP results (see text); the age (actually age range) corresponding to a given sensibility, $t_{\lambda,x\%}$ can be directly compared with the limits quoted in Table 2 for the different luminosities. In ascending ages each set of two curves correspond to $Q(H)$, GALEX/FUV and NUV, and SDSS/u, g, r, i and z. These curves can be also interpreted as the evolution of synthesis models under a constant SFR assumption, modulus the normalization factor.

3.3. SSP luminosity evolution computed by synthesis models

1. Once we have used suitable examples to manage the characterization of the evolution of SSP luminosities and estimate some numbers based in an approximate formulation of the problem, let's examine what the explicit computation of $\ell_{\lambda,\mathrm{IMF}}(t_*)$ provides. Inevitably, it implies the use of evolutionary synthesis codes to perform the detailed numerical computations, and the result becomes dependent of the details of the used code (interpolations, numerical methods, ingredients). To overcome such situation, we have compiled the results of 13 different synthesis codes/stellar population results[4] which results are public available. The models includes different atmosphere models[5] and evolutionary tracks/isochrone sets[6]; neither binaries, rotation or evolution with enhanced mass loss rates has been considered. All models assume metallicities between 0.020 and 0.019, and use (or had been transformed to) a Salpeter (1955) IMF in the mass range 0.01-100 $M_\odot$ (the impact of variations of the IMF slope at low mass does not affects the present results; we note that some models has been computed with a $m_{\mathrm{up}} = 120 M_\odot$, which has been taken into account in the censorship process, see below). No nebular continuum neither emission lines or attenuation effects have been taken into account.

We have use the computed low resolution spectral energy distribution (SED) provided by each model, to obtain the fluxes in $Q(H)$, GALEX/FUV and NUV bands, and SDSS/u, g, r, i, and z bands[7]; we have crosschecked that our results are coincident with the fluxes in these bands when provided by the modeler (and exception are results from CMD 2.0 server which provides the fluxes in all considered bands, except $Q(H)$, but not the corresponding SEDs). After a censorship process[8], we have obtain the upper and lower envelopes from the censored set of models. Then, we define a reference SSP luminosity evolutuion $\ell_{\lambda,\mathrm{IMF}}(t_*)$ by the linear mean value between both envelopes. Details are presented in a companion paper (Cerviño et al. 2016 in prep.).

2. The resulting ages where the sensitivity to the luminosity evolution of the SSP $\ell_{\lambda,\mathrm{IMF}}(t_*)$ reach a x% value of the total sensitivity, $t_{\lambda,x\%}$, and $-\log C_\lambda$ values obtained for $t_{\mathrm{age}} = 13$ Gyr are shown in Table 2. Nominal values corresponds to the reference model and the values corresponding to the upper and lower envelopes (i.e. the admisible range for where any public model is enclosed) is quoted in brackets. The age limits quoted in Table 2 can be also obtained from Fig. 2 where we show the evolution of the sensitivity of the SSP luminosity $\ell_{\lambda,\mathrm{IMF}}(t_*)$ with the age using the upper and lower envelopes of SSP results (being each of the envelopes normalized to its corresponding value). This curves can be also interpreted as the evolution of synthesis models under a constant SFR assumption, modulus the normalization factor. The figure shows how the dispersion in the results of different synthesis models and models ingredients propagates in $t_{\lambda,x\%}$ values (or in the resulting evolution under a constant SFR assumption).

The values obtained in Table 2 are comparable with $t_{\lambda,90\%}$ provided in table 1 of Kennicutt & Evans (2012) based in computations by Hao et al. (2011) and Murphy et al. (2011), although we obtain lower $t_{\lambda,90\%}$ values. This is a surprising result given that we use a quite larger t_{test}; although t_{age} and our SSP calibration includes the emission of stellar components. which are

[4] The used modelas are: STARBUST99 (Leitherer et al. 1999, 2014), GALEV (Kotulla et al. 2009), GALAXEV (Bruzual & Charlot 2003, version 2012), PEGASE2.0 (Fioc & Rocca-Volmerange 1997, 1999), POPSTAR (Mollá et al. 2009; Martín-Manjón et al. 2010; García-Vargas et al. 2013), FSPS (Conroy et al. 2009, 2010; Conroy & Gunn 2010), GALADRIEL (Tantalo & Chiosi 2004), BPASS (Eldridge & Stanway 2009, 2012, in its single star version), SED@ (Mas-Hesse & Kunth 1991; Cerviño & Mas-Hesse 1994; Cerviño et al. 2002), models provided by C. Maraston (Maraston 1998, 2005) and A. Buzzoni (Buzzoni 1989) with different Horizontal brach morphologies, models from BATSI web server including different α-enhancement factors (Percival et al. 2009; Pietrinferni et al. 2009; Salaris et al. 2010), and models from CMD 2.0 web server (Padova models, Girardi et al. 2002, 2008; Marigo et al. 2008). The web address of the models can be found in `http://sedfitting.org`.

[5] Atmosphere models includes: grids by Kurucz (1991); Castelli et al. (1997), different versions of BASEL libraries (Lejeune et al. 1997, 1998; Westera et al. 2002) for normal stars, the grids by Smith et al. (2002), Schmutz et al. (1992), and COSTAR (Schaerer & de Koter 1997) for massive and WR stars, and Planck functions and Rauch (2003) models for white dwarfs (WD).

[6] The tracks/isochrones used by the different models models are: Geneva tracks (Schaller et al. 1992), Padova tracks (Bertelli et al. 1994; Girardi et al. 2000; Marigo & Girardi 2007), BATSI tracks (Pietrinferni et al. 2004, 2006; Cordier et al. 2007; Percival et al. 2009; Pietrinferni et al. 2009; Salaris et al. 2010), and Paczyński (1970); Paczynski (1975); Bloecker (1995); Vassiliadis & Wood (1994) for post-AGB/WD evolution.

[7] Filter transmission curves has been taken from the spanish virtual observatory, SVO, server at `http://svo2.cab.inta-csic.es/theory/fps3/`

[8] Roughly, we discard the age ranges of models which shows serious discrepant results from the overall behavior of the ensemble, specially when such discrepancy is reported by the absence of particular evolutionary phases, or when the discrepant age range is outside the modeler expertise (which inferred from the age range where modelers shows their results in refereed journals).

index	$t_{\lambda,99\%}$ 10^6 yr	$t_{\lambda,95\%}$ 10^6 yr	$t_{\lambda,90\%}$ 10^6 yr	$t_{\lambda,80\%}$ 10^6 yr	$t_{\lambda,50\%}$ 10^6 yr	$-\log C_\lambda$
$Q(H)$	8.7 (7.6- 9.5)	5.3 (4.5- 5.7)	4.2 (3.6- 4.6)	3.1 (2.8- 3.3)	1.7 (1.5- 1.8)	52.93 (52.82- 53.02)
FUV	303 (266- 330)	141 (117- 156)	77 (61- 89)	31 (24- 37)	6 (5- 6)	39.99 (39.93- 40.05)
NUV	1481 (1445- 1508)	335 (310- 353)	166 (149- 177)	64 (54- 72)	8 (8- 9)	39.63 (39.55- 39.69)
index	$t_{\lambda,99\%}$ 10^9 yr	$t_{\lambda,95\%}$ 10^9 yr	$t_{\lambda,90\%}$ 10^9 yr	$t_{\lambda,80\%}$ 10^9 yr	$t_{\lambda,50\%}$ 10^9 yr	$-\log C_\lambda$
L_{bol}	12.31 (12.27- 12.32)	9.67 (9.65- 9.71)	6.96 (6.96- 6.96)	3.30 (3.31- 3.29)	0.13 (0.10- 0.15)	43.68 (43.62- 43.74)
u	11.29 (11.31- 11.29)	6.60 (6.60- 6.61)	3.47 (3.45- 3.49)	1.12 (1.13- 1.12)	0.08 (0.09- 0.08)	39.36 (39.29- 39.42)
g	12.25 (12.29- 12.24)	9.65 (9.70- 9.59)	7.15 (7.17- 7.13)	3.81 (3.78- 3.84)	0.55 (0.55- 0.54)	39.48 (39.42- 39.54)
r	12.52 (12.53- 12.50)	10.69 (10.77- 10.63)	8.75 (8.85- 8.68)	5.79 (5.84- 5.75)	1.37 (1.35- 1.39)	39.40 (39.32- 39.46)
i	12.59 (12.60- 12.57)	10.95 (11.03- 10.89)	9.16 (9.29- 9.07)	6.31 (6.44- 6.23)	1.70 (1.76- 1.67)	39.31 (39.23- 39.38)
z	12.62 (12.64- 12.60)	11.12 (11.20- 11.06)	9.43 (9.60- 9.31)	6.67 (6.90- 6.51)	1.91 (2.09- 1.79)	39.25 (39.15- 39.33)

Table 2. Ages where the sensitivity to $\ell_{\lambda,\mathrm{IMF}}(t_*)$ reach a x% value of the total sensitivity, $t_{\lambda,x\%}$, for 99, 95, 90, 80 and 50% and all luminosities used in this work. Last column is the C_λ value as defined in Eq. 8. The units of C_λ are in erg s^{-1} Å^{-1} M$_\odot^{-1}$ yr for the standard photometric systems and photons s^{-1} M$_\odot^{-1}$ yr for $Q(H)$. Values in parenthesis corresponds to the use of upper and lower envelope of $\ell_{\lambda,\mathrm{IMF}}(t_*)$ obtained from our calibration of SSP models.

not included in the models used by Hao et al. (2011); Murphy et al. (2011); Kennicutt & Evans (2012). This difference would be due to the use of Meynet et al. (1994) evolutionary tracks with enhanced mass loss rates by the mentioned authors, the default in STARBUST99 previous the release including rotation, which are not included in our censored calibration (see Cerviño et al. 2016 in prep. for more details).

The variability due to the use of different synthesis models in our compilation quoted in Table 2 is quite lower than the 20% usually quote in the literature. However, such scatter corresponds to an optimistic situation since our compilation is restricted to the evolutionary tracks used in common synthesis codes. A detailed analysis of possible uncertainties due to evolutionary tracks which are not included in our compilation can be found in Martins & Palacios (2013). In addition, the compilation only include solar metallicity models, so, again, the quoted uncertainties are lower limits since does not consider metallicity variations.

3. Figure 3 shows the $\ell_{\lambda,\mathrm{IMF}}(t_*)$ sensitivity curves once normalized to its integral over 13 Gyr, which is the transmission over which the SFH is seen by the corresponding luminosity. The figure allows to compare directly with the sensitivity to the SFH for each possible integrated luminosity independently if it is used as a recent SFH proxy or not. To simplify the discussion, we have only used the reference model described before. The left panel in the figure shows the sensitivity in linear scale form 0 to 10 Myr, and right panel shows the sensitivity in logarithm scale in the whole age range. In the following paragraphs we compare the four groups of indices with different behavior, which are $Q(H)$, UV indices, U (SDSS/u), and optical/IR indices.

$Q(H)$ is clearly the most sensitive index to the younger component of the SFH. Even more, the sensitivity peaks at ages lower than 1 Myr, hence, in first approximation, it almost reproduce the present value of the SFH. In addition, its sensitivity to the recent SFH (t_{now} − 3Myr) is about a factor 3 larger than any other index. It is the less sensitive index to the SFH at ages t_{now} − 10Myr up to ages older than 1 Gyr, where the sensitivity of GALEX/FUV is lower. The dynamic range of the sensitivity to the SFH at different ages covers 6 decades (more than 3 decades in the first 10 Myr), hence, it is quite stable[9] to large scale variations in the SFH at ages older than 50 Myr. In a relative comparison with the other indices (i.e. where the different sensitivities crosses each other), $Q(H)$ is more sensitive to the SFH at ages lower ∼4 Myr than GALEX filters, ∼5 Myr than u and ∼7 Myr than optical bands.

The indices based in the UV, GALEX/FUV and NUV, have a quite similar transmission, although GALEX/FUV is a bit more sensitive to the young component up to ages around 8 Myr than GALEX/NUV, and GALEX/NUV is more sensitive than GALEX/FUV for the SFH at ages longer than 100 Myr. The peak of the sensitivity is around 3 Myr (the value of t_{MS} at the given metallicity), being the sensitivity of both indices broader than $Q(H)$ and extending with an apreciable sensitivity for ages longer than 10 Myr. Both indices have almost equivalent sensitivity to the SFH in the range 8 to ∼50 Myr. At older ages, and specially at ages older than ∼ 300 Myr the sensitivity of GALEX/FUV drops abruptly, whereas the one of GALEX/NUV declines more smoothly. The dynamic range of the sensitivity at different ages covers almost 5 decades (more than 3 decades in the first 500 Myr), and, as in the case of $Q(H)$, both indices are quite robust to large scale variations of the SFH, although at a time scale much more larger that the one associated to $Q(H)$.

The case of U band is and intermediate case between optical and UV bands. It is about a factor 2 less sensitive to the recent SFH than UV filters but still a factor 2 lager than g; however, the sensitivity to the SFH after 50 Myr is larger than the UV bands (reaching factors larger than 10 at ages large than 2-3 Gyr). So, although it looks to works correctly as a recent SFR index using the standard methodology when tested over sort time-scales (i.e. t_{test} up to ∼ 100 Myr), it behaves more like optical colors a larger ages. Actually, the slope of the sensitivity with time is quite similar to −1, which is the limiting case where the sensitivity to young and old components of the SFH are similar. The dynamic range of the sensitivity is a bit larger than 3 decades over the whole age range, and, as quoted before, more sensitive to large scale variations of the SFH than the previous indexes.

Larger wavelengths (g, r, i, and z bands), still shows a important sensitivity to the recent SFH, however, their dynamic range is lower than 3 decades, hence, much more affected by large scale variations on the SFH. In addition, the sensitivity curves of all optical bands intercept each other near 1 Gyr. Among them, the sensitivity of r, i and z bands are quite similar, which implies in a first approximation that they would provide redundant information in any SFH inference, specially after the first 10 Myr.

[9] Numerical computations shows that, assuming t_{age} = 13Gyr, the old component of exponential decay and delayed SFH with $\tau > 3$Gyr affects the index in less than 10% (Cerviño et al. 2016b in preparation).

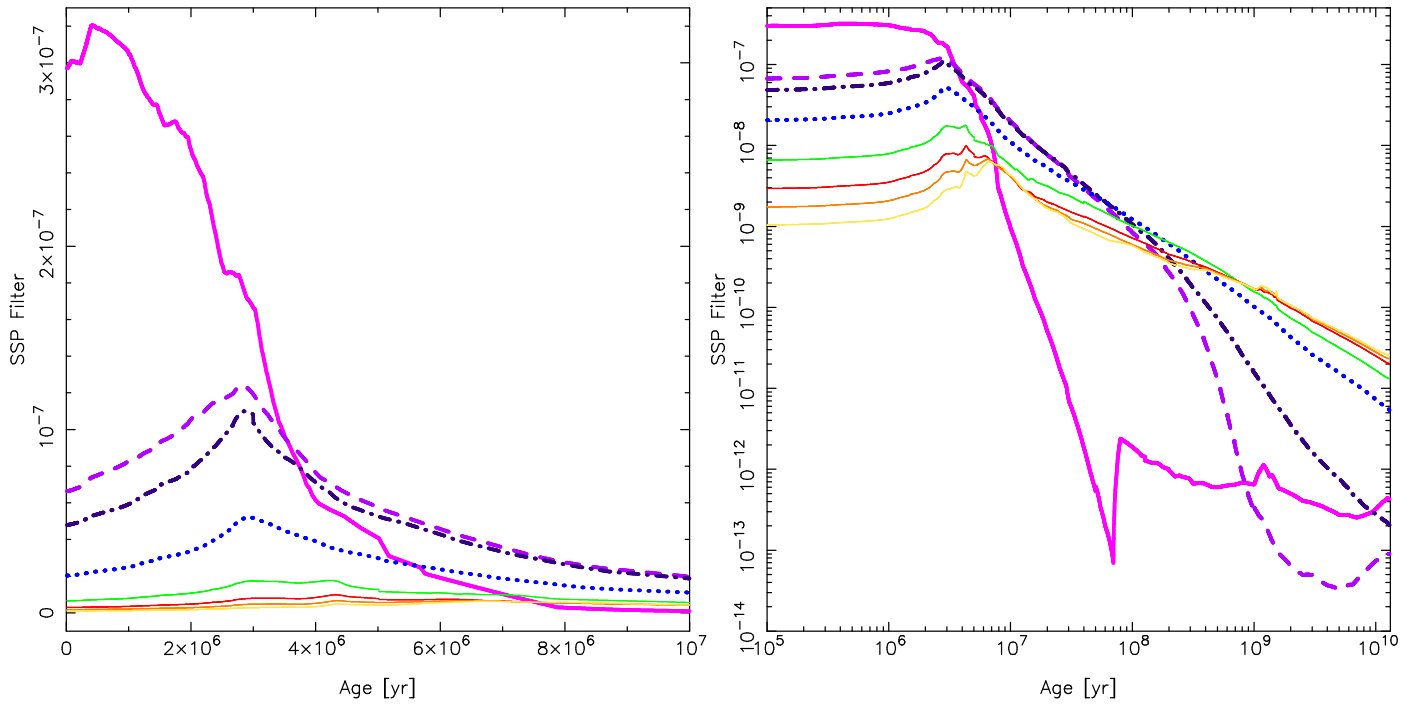

Fig. 3. SSP luminosity evolution $\ell_{\lambda,\mathrm{IMF}}(t_*)$ as SFH sensitivity curve (i.e. once normalized to the integral of the SSP over the age of the system, 13 Gyr in our case). The left panel shows the sensitivity curve in linear scale from 0 to 10^7 yr, and the right panel the sensitivity curve in log-log scale in the whole age range. In descending order at young ages the curves correspond to $Q(H)$, GALEX/FUV and NUV, and SDSS/u, g, r, i and z.

	$\mathcal{B}-$ NUV [AB]	$t_{*,\mathcal{B}-\mathrm{NUV}}$ [Myr]	$\mathcal{B}-u$ [AB]	$t_{*,\mathcal{B}-u}$ [Myr]	$\mathcal{B}-g$ [AB]	$t_{*,\mathcal{B}-g}$ [Myr]	$\mathcal{B}-r$ [AB]	$t_{*,\mathcal{B}-r}$ [Myr]	$\mathcal{B}-i$ [AB]	$t_{*,\mathcal{B}-i}$ [Myr]	$\mathcal{B}-z$ [AB]	$t_{*,\mathcal{B}-z}$ [Myr]
FUV$-\mathcal{R}$	−0.02	(7 - 50)	0.25	(40-60)	1.16	(80)	1.55	(∼120)	1.74	(∼150)	1.98	(∼150)
NUV$-\mathcal{R}$			0.27	(40-50)	1.18	(100)	1.57	(∼180)	1.76	(∼200)	2.00	(∼200)
$u-\mathcal{R}$					0.91	(∼180)	1.30	(∼400)	1.49	(∼400)	1.73	(∼400)
$g-\mathcal{R}$							0.39	(∼700)	0.59	(∼700)	0.82	(∼700)
$r-\mathcal{R}$									0.19	(400 - 1000)	0.43	(400 - 1000)
$i-\mathcal{R}$											0.24	(400 - 4000)

Table 3. Colors obtained from the normalized $\langle\mathcal{SFR}\rangle_\lambda$ calibration in magnitudes in the AB system. The age where each sensitivity curve cross each other in Myr units is quoted in parenthesis. In the case of r, i and z combination of colors there is an additional crossing age in the 7- 13 Myr range not quoted in the table.

3.3.1. Relative time-scales and $\langle\mathcal{SFR}\rangle_\lambda$ corrections

1. In the previous section we showed the difficulties to define any characteristic time scale Δt which allows transform an observed $\langle\mathcal{SFR}\rangle_\lambda$ into $\langle\mathcal{SFR}\rangle_{\Delta t}$ or, at least obtain an age interval over the SFH has been averaged. We can choose a characteristic time scales associated with the evolution of SSP luminosities $\ell_{\lambda,\mathrm{IMF}}(t_*)$ (e.g. $\langle t_*\rangle_\lambda$, any $t_{\lambda,x\%}$ or any other related time scale), but they do not provides directly the time range over the actual SFH is averaged neither $\langle t_*\rangle_{\lambda,\psi}$, or $t_{\lambda,x\%,\psi}$, which depend on the unknown functional form of the overall SFH.

However, by the comparison of the $\langle\mathcal{SFR}\rangle_\lambda$ obtained for different indices (including optical ones), we can obtain relative time scales of the SFH whatever its functional form. It is, we cannot define the time interval over $\psi(t)$ is averaged, but we can establish some characteristic times which, once compared with an associated color, allows to establish the relative strength of $\psi(t)$ after and before such time. As result, although we can not correct $\langle\mathcal{SFR}\rangle_\lambda$ to obtain $\langle\mathcal{SFR}\rangle_{\Delta t}$, we can establish if $t_{\lambda,x\%,\psi}$ (which is unknown) is larger or lower than $t_{\lambda,x\%}$. In the following we assume the general result that the sensitivity to the recent SFR increases at lower wavelengths.

2. Relative time scales are given by the intersection of the different transmission curves: Let us assume two indices $C_\mathcal{B}$ and $C_\mathcal{R}$ where $\mathcal{B}$ and $\mathcal{R}$ refers to bluest or redder bands used to define the color, or in terms of the transmission curves, more sensitive to the young ($\mathcal{B}$) or old ($\mathcal{R}$) component of the SFH. First, let us define a reference color $(\mathcal{B}-\mathcal{R})_{\mathrm{ref}}$ obtained from the corresponding C_λ values (i.e. obtained at t_{age}). Second, let be $t_{*,\mathcal{BR}}$ the intersection age of the two sensitivity curves. Given that $\psi(t)$ is independent of the transmission curves, an extinction-corrected observed color bluer than $(\mathcal{B}-\mathcal{R})_{\mathrm{ref}}$ implies that $\psi(t)$ have a larger contribution in the age region where the blue index is more sensitive, it is, at ages lower than $t_{*,\mathcal{BR}}$. In such situation, we can also assure that any of the time scales $\langle t_*\rangle_\lambda$ or $t_{\lambda,x\%}$ are upper values of the actual $\langle t_*\rangle_{\lambda,\psi(t)}$ or $t_{\lambda,x\%,\psi(t)}$ values. It is, from the variation of the color $(\mathcal{B}-\mathcal{R})$ with respect to $(\mathcal{B}-\mathcal{R})_{\mathrm{ref}}$ we can obtain information about the relation between $\langle t_*\rangle_\lambda$ (obtained theoretically) and $\langle t_*\rangle_{\lambda,\psi(t)}$ (the cuantity we are interested in).

This case can be viewed as the comparison of the colors obtained from a constant SFH over all the possible age range

with any other possible SFH. The improvement is that we have take advantage of the functional form of the different normalized $\ell_{\lambda,\mathrm{IMF}}(t_*)$ curves and their intersection in the time axis to characterize the deviations from a constant SFH.

Let us illustrate it with an example: $Q(H)$ is not directly an observable but it is directly proportional to the Hα emission line with a conversion factor of 1.36×10^{-12}, (assuming Case B recombination and no scape of ionizing photons, hence an upper limit of $L(\mathrm{H}\alpha)$). Using the flux in r band as a representation of the continuum near Hα, the resulting equivalent width of Hα in emission obtained from the respective $C_{Q(H)}$ and C_r values is EW(Hα) ~ 45 Å. Note that in this computation the value of r is a lower limit since we are not considering nebular contribution to r (which is around 40% at young ages Mas-Hesse & Kunth 1991), so 45 Å is a maximum value. Since the sensitivity curve of $Q(H)$ and r intercepts at around 7 Myr, the SFH in a system with EW(Hα) > 45 Å, the actual SFH must be stronger (in reference to a constant SFH) in the last 7 Myr. A larger value of EW(Hα) implies that recent SFH is more concentrated at younger ages, hence the mean luminosity weighted age associated to the actual SFH) $\langle t_* \rangle_{\psi(t)}$ is lower than the mean luminosity weighted age associated to a constant SFH) $\langle t_* \rangle$, hence the recent SFH is bursty-like (at least in first approximation). However, the inverse reasoning of a recent SFH extending in time for ages larger than 7 Myr if EW(Hα) < 45 Å is not true since it can be due to the enhanced of the r due to nebular emission we have not consider, the leaking of ionizing photons, and/or in combination that the SFH at ages larger than 7 Myr is more relevant to the integrated $L(\mathrm{H}\alpha)$. Whatever the case, the EW(Hα) value and the normalized $\ell_{\lambda,\mathrm{IMF}}(t_*)$ curves provide additional information about the recent SFH which helps to interpret the quantity $\langle \mathcal{SFR} \rangle_{Q(H)}$ independently of the SFH itself. Equivalently FUV-NUV colors larger (or lower) than -0.02 or NUV-r larger or lower than 1.57 provides additional constraints about the time scales around 7-50 Myr and 140 Myr respectively (c.f. Tab. 3).

3. In the previous paragraph we had focused in provide a time-scale to the $\langle \mathcal{SFR} \rangle_\lambda$ obtained from data of a single system. In the case of a large set of systems (e.g. survey studies), the principal interest is not the time scale associated to the $\langle \mathcal{SFR} \rangle_\lambda$ in each system, but to the comparison of $\langle \mathcal{SFR} \rangle_{\Delta t}$ where Δt is equal (or at least similar) for all the systems in the set. In such case, the comparison of the observed color $(\mathcal{B}-\mathcal{R})$ with respect to $(\mathcal{B}-\mathcal{R})_{\mathrm{ref}}$ provide a hints about the correction to transform $\langle \mathcal{SFR} \rangle_\lambda$ in $\langle \mathcal{SFR} \rangle_{\Delta t}$.

4. However, although the idea is formally correct, this method only provide first order time scales. As an example the GALEX/FUV and NUV sensitivities crosses each other nominally at 17 Myr, but the sensitivity is almost identical (with variations lower than ±10%) in the age range from 7 to 50 Myr[10]. In addition, the present sensitivity curves have been obtained assuming that all stars formed in over the last 13 Gyr has solar metallicity, which neglects metallicity evolution of different populations. Finally, we had not consider extinction effects which affects the results of SFR inferences and which had been studied by different authors. Being quoted the previous cautions, we show in Table 3 the $(\mathcal{B}-\mathcal{R})_{\mathrm{ref}}$ colors associated to the different C_{ind} values of table 2 when expressed AB magnitudes, and the approximate ages (obtained by eye-inspection of Fig. 3) where the sensitivity curves cross each other.

[10] These numbers has been obtained without take into consideration the uncertainties in the our calibration of synthesis models, which introduces an additional scatter in the reliable time scales

5. Finally, we stress that present results are independent of the SFH, and apply also to the extreme SFH of instantaneous burst of star formation. In the case of EW(Hα), an EW(Hα) > 45 Å roughly corresponds to a burst (i.e. SSP) older than 7 Myr. A direct implication is that, in practice, we can interpret any fit of colors obtained from SFR indices to SSP results as a hint about the different time-scales each index applies. Although outside the scope of this paper, such alternative vision about what provide a SSP fit, even in the case that we know a priori that our studied system is not a single burst of star formation, can be potentially exploited in SFH inferences obtained from the integrated spectra/photometry of any stellar system.

4. Discussion by comparison with other works

The principal result of this work is a change of perspective about what is obtained in recent SFH inferences. This result has not a great impact on the final values of the standard SFR calibrations ($Q(H)$ and UV indices) which are only affected in a few percent, but it clearly affects the case of the U band and allows to introduce optical colors as a cross-checking about the time scales associated to SFR inferences. Although we have obtained some numbers, our approach is rather qualitative. However such quantitative results allow to put in a firm theoretical bases some of recent results related with recent SFH inferences. So, instead to perform quantitative test, we use the results by other authors to discuss our main results.

1. *Extending Boquien et al. (2014) results.* The first result refers to the age t_{test} that should be used to calibrate recent SFH indices. As it has been shown, the best t_{test} value is the age of the galaxy under consideration t_{age} (which actually is redshift dependent). It applies even for SFR inferences in regions inside galaxies, since it is always posible the contribution of an old stellar population.

Taken that into consideration, we can extend the results obtained by Boquien et al. (2014) about the use of any particular t_{test}: Boquien et al. (2014) used the SFH from MIRAGE simulations (Perret et al. 2014) covering ages up to 780 Myr and compare the instantaneous SFH with the evolution of $\langle \mathcal{SFR} \rangle_\lambda$ for different indices ($Q(H)$, FUV, NUV and u) obtained by including the simulated SFH in stellar population synthesis codes. Their main finding is that the calibration of the SFR is age dependent (i.e. in line with our claim that the best t_{test} is the age of the system), and they propose to use of a t_{test} of at least 1 Gyr instead the typical one of 100 Myr when a fixed value of t_{test} is used. We note that 1 Gyr is nearby the maximum age considered by their used SFH.

However, we can also establish that, extending the simulations over larger age range, a calibration over t_{test} = 1 Gyr will produce again biased results (see Sect. 3.2). In particular, the case of the u band is specially ill defined as SFR index: since it evolves as a power law with slope close to the limiting value of -1, it would looks to be a good SFR index for any fixed age t_{test}, but it overestimate the true SFR if the system is older than t_{test}.

In addition, Boquien et al. (2014) studied the delay between $\psi(t)$ and the $\langle \mathcal{SFR} \rangle_\lambda$ produced by the models at the given t. They found that $\langle \mathcal{SFR} \rangle_{Q(H)}$ follows $\psi(t)$ with delay of around 1 Myr, whereas the other $\langle \mathcal{SFR} \rangle_\lambda$ indices have typical delays of few Myr, although their plots (e.g. Figs. 6 and 8) shows that there is a delay plus an smoothness effect. Such results are,again, fully consistent with our analysis where $\langle \mathcal{SFR} \rangle_\lambda$ is a filter over $\psi(t)$.

2. *Johnson et al. (2013) results.* A second result is to break the artificial duality in the use of t_{test}, that is implicitly assumed to be related with a possible value of t_{ind}, i.e. the time scale over

the SFR is averaged. We have shown that such time-scales can not be obtained, since it depends on the particular SFH, which is unknown. Ever more, to impose *ad hoc* a constant SFH to obtain a t_{ind} value produces ill-defined questions, since t_{ind} is intrinsically undefined. This situation is clearly illustrated in Johnson et al. (2013) who, making use of SFH obtained from CMD, computed the SFH dependent $t_{uv,80\%,\psi(t)}$ values from a sample of 50 nearby dwarf galaxies (where *uv* refers to both FUV and NUV). They find that depending on the SFH such values ranges from few Myr up to 10 Gyr, being this value linearly correlated with the NUV-*r* color, so the inferred $\langle \mathcal{SFR} \rangle_{uv}$ can not be univocally related with any SFR time-scale.

We stress that such result is not a problem of the calibrations of the recent SFR, but rather with the interpretation of what we would like a $\langle \mathcal{SFR} \rangle_{uv}$ value provides, but it does not. Again, the calibrations are correct (when $t_{test} = t_{age}$, a question also addressed partially in Johnson et al. 2013), but such calibrations does not provide directly a time scale; it is required additional information (as optical or IR colors) to provide a recent SFR time scale (actually information about the global SFH). As an example, our computations produce a NUV-*r* = 1.57 (c.f. Tab. 3) with a characteristic age associated to such color around 180 Myr. In previous section we stated that a bluer (redder) NUV-*r* indicates that the SFH is more concentrated at younger (older) ages, which translate to a lower (larger) value of any $t_{uv,x\%,\psi(t)}$ characteristic age; an effect which is in agreement with Johnson et al. (2013) findings.

However, we note that our explanation of the correlation between NUV-*r* and $t_{uv,80\%,\psi(t)}$ found by Johnson et al. (2013) is only valid for NUV-*r* color bluer or near a NUV-*r* value of 1.57, but it cannot extended to extreme (much redder than 1.57) NUV-*r* colors. That is, we only explain the bluer part of the correlation found by Johnson et al. (2013), but it is required a more complete study about the impact of the SFH at old ages (roughly, larger than 1 Gyr) to find a satisfactory explanation of the correlation.

3. *Simones et al. (2014) results.* In the case of star forming regions inside a galaxy we have a similar situation of a correlation of different colors with any SFR averaged over a predefined time-scale, although with some subtle differences: (a) Stellar populations formed at old ages will be spread over all the volume of the galaxy, hence, it is expected that $\psi(t)_{\rm region}$ that would be obtained from particular blue region will have a lower contribution from the older stellar populations (modulus the position in the galaxy). (b) Although the increasing of resolution would optimize a $\psi(t)_{\rm region}$ inference, it also implies a reduction in the amount of stars which contributes to the total luminosity, so an increasing on the uncertainty of the inferences obtained from the integrated luminosity (the so called IMF sampling effects, although stellar luminosity function sampling effects is a more correct description; see Cerviño & Luridiana 2004, 2006; Cerviño 2013, and references therein for a extensive discussion on the subject).

Let us illustrate both situations using the work by Simones et al. (2014), who analyzed the CMDs obtained from the Panchromatic Hubble Andromeda Treasury data (Dalcanton et al. 2012) to obtain the corresponding SFH in the last 500 Myr, and extinction of 33 FUV-bright regions in M31 and use them to test the reliability of FUV as an SFR index at small scales.

The authors provides the SFH of each region; from it, they obtain the SFH averaged over the last 100 Myr ($\langle SFR \rangle_{100}$), the age where the SFH has a peak, $\mathrm{Age}_{\rm peak}$, and the ratio between the mass of stars formed in the $\mathrm{Age}_{\rm peak}$ over the mass of star formed in the las 100 Myr, $M_{\rm peak}/M_{100}$. In addition, they use the SFH as input of a synthesis model to obtain the integrated luminosity in GALEX/FUV and $(\mathrm{FUV-NUV})_{\rm mod}$ color, and the corresponding $\langle \mathcal{SFR} \rangle_{fuv,\rm mod}$ using the standard calibration. Finally, they use their extinction solution and apply it to GALEX data to obtain the extinction corrected FUV flux and the corresponding $\langle \mathcal{SFR} \rangle_{fuv,\rm obs,0}$. One of the advantages of this paper is that, besides their detailed analysis, the authors provide a plot the SFHs obtained from each of the studied region as well as different set of tables including the computed quantities, from which not tabulates values, as the extinction corrected $(\mathrm{FUV-NUV})_{\rm obs,0}$ color, can be obtained. From a comparison of the ratio $\log \langle \mathcal{SFR} \rangle_{fuv} / \langle SFR \rangle_{100}$ as a function of the area covered by the region, and using observed and modeled $\langle \mathcal{SFR} \rangle_{fuv}$ values, they claim that the extinction corrected FUV fluxes are, on average, consistent with $\langle SFR \rangle_{100}$ within a 1-σ scatter, which is related with the discrete sampling of the IMF and the high time variability on the recent SFH.

Again we can extend the conclusions of Simones et al. (2014) taking advantage of the present study. In Fig. 4 we show the ratio $\log \langle \mathcal{SFR} \rangle_{fuv} / \langle SFR \rangle_{100}$ vs. the FUV-NUV color obtained from Simones et al. (2014) by the use of the SFH implemented in synthesis models (left), and obtained from the observed data once corrected from extinction (right). The color of the different points shows the $\mathrm{Age}_{\rm peak}$ value, and the size of each point is proportional to $M_{\rm peak}/M_{100}$.

When synthesis models are used and sampling effects are neglected, there is a clear correlation between $\log \langle \mathcal{SFR} \rangle_{fuv} / \langle SFR \rangle_{100}$, the FUV-NUV color and $\mathrm{Age}_{\rm peak}$, which is stronger for larger $M_{\rm peak}/M_{100}$. The combination of $\mathrm{Age}_{\rm peak}$ and $M_{\rm peak}/M_{100}$ are a measure about the concentration of the SFH at different ages, so the results of their simulations are consistent our prediction about the dependence of $\langle \mathcal{SFR} \rangle_{\lambda}$, $\langle SFR \rangle_{\Delta t}$, and the color of the system. We note that the Simones et al. (2014) conclude that the dispersion on $\langle \mathcal{SFR} \rangle_{fuv} / \langle SFR \rangle_{100}$ are due to to the the variability of the recent SFH, but they are not aware about the correlation shown here and that such correlation can be used to reduce such scatter.

In the case of use observational data, sampling effects produce that the correlation of $\log \langle \mathcal{SFR} \rangle_{fuv} / \langle SFR \rangle_{100}$ and the FUV-NUV color disappear. This result is not surprising since only 1 cluster in their analysis reach an amount of gas transformed into stars in the last 100 Myr larger than 10^5 $M_\odot$, and such value is roughly the lowest limit quoted by Cerviño & Luridiana (2004) to model a system safely in UV-Optical bands (i.e. without extreme sampling effects where the mean value obtained by synthesis models lost its predictive power). However, there is still a clear tendency of found lower values of $\langle \mathcal{SFR} \rangle_{fuv} / \langle SFR \rangle_{100}$ in clusters where the SFH has a larger star formation concentration at older ages and viceversa. It is, $\langle \mathcal{SFR} \rangle_{fuv} / \langle SFR \rangle_{100}$ still depends on the age range where the actual SFH is more concentrated.

5. Conclusions

In this work we had translated the statements quoted in the constant SFR approximation presented by Kennicutt (1998), which requires synthesis models for its calibration, to the intrinsic algebra of synthesis models in order to capture the principal characteristics of such approximation which allows to obtain reasonable SFR inferences. The results obtained from this study are:

1. When expressed in terms of SFH estudies, any integrated luminosity can be (and should be) considered as the result of filtering the SFH using SSP.

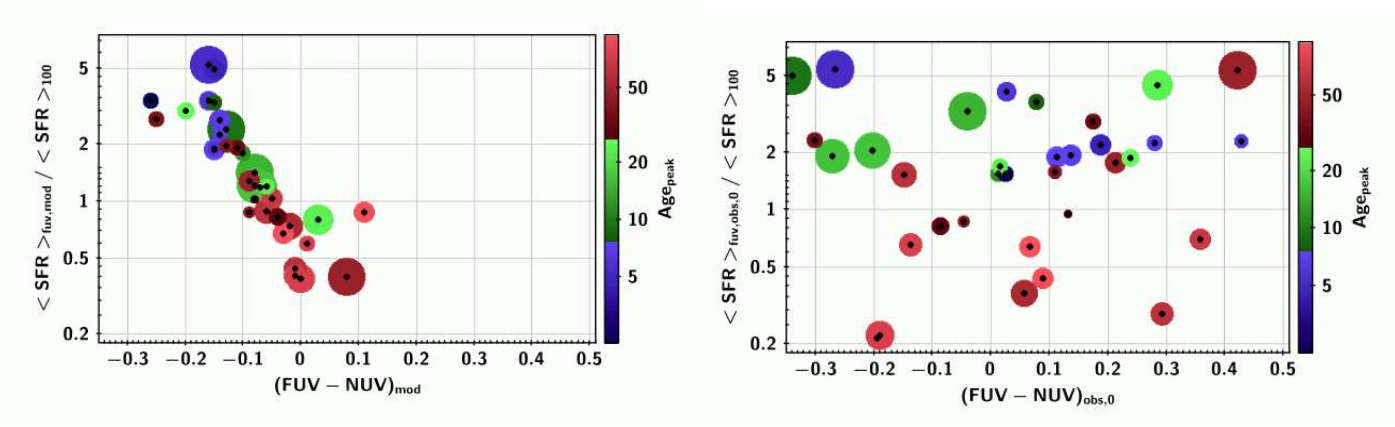

Fig. 4. Ratio of $\log \langle \mathcal{SFR} \rangle_{fuv} / \langle SFR \rangle_{100}$ vs. the FUV-NUV color obtained from Simones et al. (2014) data by the use of the SFH implemented in synthesis models (left), and obtained from the observed data once corrected from extinction (right). The color of the different points shows the $\mathrm{Age}_{\mathrm{peak}}$ value, and the size of each point is proportional to $M_{\mathrm{peak}}/M_{100}$.

$$\begin{aligned} \langle \mathcal{SFR} \rangle_{\varphi_\lambda(t)} &= \int_0^{t_{age}} \psi(t)\, \varphi_\lambda(t) dt = \\ &= \frac{\int_0^{t_{age}} \psi(t)\, \ell_{\lambda,\mathrm{IMF}}(t_{age} - t)\, \mathrm{d}t}{\int_0^{t_{age}} \ell_{\lambda,\mathrm{IMF}}(t_*)\, \mathrm{d}t_*} \\ &= \frac{\mathcal{L}_\lambda(t_{age})}{\int_0^{t_{age}} \ell_{\lambda,\mathrm{IMF}}(t_*)\, \mathrm{d}t_*} = C_\lambda \times \mathcal{L}_\lambda(t_{age}), \end{aligned} \tag{15}$$

being C_λ, the SFR calibration coefficient, a normalization factor of SSP models.

2. Given that all the SFH of the system must be taken into account, the most reliable choice of the age to be used in the calibration is the system age, t_{age} (roughly 13 Gyr at $z = 0$). This calibration varies with the redshift provided correct the assumption that all galaxies had been formed at a given cosmic epoch and independently of their posterior SFH.
3. The time evolution of the SSP luminosity $\ell_{\lambda,\mathrm{IMF}}(t)$ from 0 to t_{age} acts like a filter over the SFH, so it is the characterization of $\ell_{\lambda,\mathrm{IMF}}(t)$ who enables us to infer recent SFR. Under this perspective, there is no requirement about the functional form of the SFH to calibrate different SFR indices; in particular, a constant SFR is not a required hypothesis. The only advantage of the a constant SFH assumption is that, if Nature had works in such a way, the resulting SFR is an exact value.
4. Using a simple, parametrization of the SSP luminosity evolution $\ell_{\lambda,\mathrm{IMF}}(t)$, and detailed synthesis models results, we found that U band is a ill-defined index to be used as a primary proxy of the SFR. It looks like primary proxies ($Q(H)$ or UV indices) when the calibration is done using small time scales, and as optical indices when used large time scales. Whatever the case such situation does not pose any problem if t_{age} is used as calibration age.
5. We had shown that the assumed requirement that the integrated luminosity reach an asymptotical or steady-state value under a constant SFR hypothesis is not needed. Actually, for the given age of the Universe, such asymptotical value is never reached. Reach the asymptotical would allow to define a practical cut-off in the sensitivity defined by $\ell_{\lambda,\mathrm{IMF}}(t)$, hence to define a characteristic time scale over the SFH is in practice averaged. Unfortunately such cut-off does not exists and characteristics time scales are dependent on the unknown SFH. The best be can do is to characterize the sensitivity to the SFH provided by $\ell_{\lambda,\mathrm{IMF}}(t)$. We have shown that the time used for the calibration must be not confused with the characteristic time scales of $\ell_{\lambda,\mathrm{IMF}}(t)$ which are strongly dependent on the wavelength. We have provide different ways to obtain such characteristic time-scales.
6. Using the $\langle \mathcal{SFR} \rangle_\lambda$ values obtained from different indices and the characterization $\ell_{\lambda,\mathrm{IMF}}(t)$ (e.g. the use of equivalent widths or colors), we can establish time ranges where the SFH have a larger contribution to the different indices, hence improve the meaning of the measure given by $\langle \mathcal{SFR} \rangle_\lambda$. The results obtained in this way are independent of the functional form of the SFH. To perform this task, it is required to calibrate all possible wavelengths (not only the standard ones of ionizing flux or UV fluxes) as established by Eq. 15.
7. We have shown that, theoretically, there should be a correlation between the SFR obtained by the calibration of a particular luminosity $\langle \mathcal{SFR} \rangle_\lambda$, the physical SFR which is the SFH averaged over a given time interval $\langle \mathcal{SFR} \rangle_{\Delta t}$ and the galaxy colors. Such correlation are present in other works in the literature, and it is generally considered has a prove of the different time scales associated to $\langle \mathcal{SFR} \rangle_\lambda$ and $\langle \mathcal{SFR} \rangle_{\Delta t}$, hence a problem to obtain $\langle \mathcal{SFR} \rangle_{\Delta t}$. We show that it is a natural result implicit in the very nature of the relation of the observed luminosity and the SFH of the system, and that it can be used to correct (or at least estimate a correction) of $\langle \mathcal{SFR} \rangle_\lambda$ to obtain $\langle \mathcal{SFR} \rangle_{\Delta t}$.

After this study we conclude that the constant SFR approximation quoted by Kennicutt (1998) actually contains deeper implications which are intrinsic to the population synthesis model algebra, but with a different wording and a few subtle changes: (1) The quoted constant SFH assumption is naturally translated to a normalization factor to express SSP results as a sensitivity curve, and it is applicable to any wavelength. (2) The steady-state (i.e. asymptotic) requirement to define reliable SFR is naturally translated to a measure of the relative sensitivity of the $\ell_{\lambda,\mathrm{IMF}}(t)$ filter to the young and old component of the SFH, and, although a desirable property, it is not a requirement to obtain information about the recent SFH. (3) Finally, the bluest, the best statement is a synthetic and operative version about the fact that, whatever the wavelength, there is a peak of sensitivity in the recent SFH age range. Since shorter wavelengths have a larger sensitivity, a blue color assures that the possible contamination from

the old component of the SFH is minimized. However such statement has a limit depending on the galaxy color and the studied system; it works for systems with colors redder than the colors associated to the calibration of $\ell_{\lambda,\mathrm{IMF}}(t)$ (or equivalently, predictions of a constant SFH over all the possible age range). In the case extreme blue colors, there is a first order correlation within the color, the obtained value of $\langle \mathcal{SFR} \rangle_\lambda$ and the actual value of $\langle \mathcal{SFR} \rangle_{\Delta t}$. It is not clear if such correlation can be used to transform $\langle \mathcal{SFR} \rangle_\lambda$ value into the desired value of $\langle \mathcal{SFR} \rangle_{\Delta t}$, but at least provides hints about over or underestimations of $\langle \mathcal{SFR} \rangle_\lambda$ with respect $\langle \mathcal{SFR} \rangle_{\Delta t}$.

As a final comment, this work has been done in an old-fashion way, preferring the use of reasonable analytical approximations as a function of suitable parameters to the use of detailed numerical computations where numerical values difficult any possible parametrization. Such kind of reasoning, although not exact, can be found in most of B. Tinsley papers, and A. Buzzoni ones who show that the key points to understand the results obtained by detailed simulations can be obtained using simple, but powerful, reasoning. As we had shown, such methodology provide hints about which kind of plots or correlations would be hidden under more elaborated numerical experiments. It is true that for some aspects (track interpolations, atmosphere models assignation, among others) synthesis models should be used as black boxes for non initiated developers, but for some purposes a simple inspection of the implicit equations in any synthesis model, and their possible solutions, is the only requirement.

Acknowledgements. We thank the referee, Rob Kennicutt, for his comments, which helped improve this paper. This work has done extensive use of TopCat software (Taylor 2005) and we acknowledge Mark Taylor for its development. This work has been supported by the Spanish Programa Nacional de Astronomía y Astrofísica of the MINECO by the projects AYA2014-58861-C3-1 (MC), and AYA2013-42781-P (SH), and partially supported by the project AYA2011-C03-01 (AB).

References

Bertelli, G., Bressan, A., Chiosi, C., Fagotto, F., & Nasi, E. 1994, A&AS, 106, 275
Bloecker, T. 1995, A&A, 299, 755
Boquien, M., Buat, V., & Perret, V. 2014, A&A, 571, AA72
Bruzual, G., & Charlot, S. 2003, MNRAS, 344, 1000
Buzzoni, A. 1989, ApJS, 71, 817
Buzzoni, A. 1995, ApJS, 98, 69
Buzzoni, A. 2002, AJ, 123, 1188
Buzzoni, A. 2002b, New Quests in Stellar Astrophysics: the Link Between Stars and Cosmology, 274, 189
Buzzoni, A. 2005, MNRAS, 361, 725
Calzetti, D. 2013, Secular Evolution of Galaxies, 419
Castelli, F., Gratton, R. G., & Kurucz, R. L. 1997, A&A, 318, 841
Cerviño, M., & Mas-Hesse, J. M. 1994, A&A, 284, 749
Cerviño, M., Mas-Hesse, J. M., & Kunth, D. 2002, A&A, 392, 19
Cerviño, M., & Luridiana, V. 2004, A&A, 413, 145
Cerviño, M., & Luridiana, V. 2006, A&A, 451, 475
Cerviño, M. 2013, New A Rev., 57, 123
Conroy, C., Gunn, J. E., & White, M. 2009, ApJ, 699, 486
Conroy, C., White, M., & Gunn, J. E. 2010, ApJ, 708, 58
Conroy, C., & Gunn, J. E. 2010, ApJ, 712, 833
Conroy, C. 2013, ARA&A, 51, 393
Cordier, D., Pietrinferni, A., Cassisi, S., & Salaris, M. 2007, AJ, 133, 468
Dalcanton, J. J., Williams, B. F., Lang, D., et al. 2012, ApJS, 200, 18
Eldridge, J. J., & Stanway, E. R. 2009, MNRAS, 400, 1019
Eldridge, J. J., & Stanway, E. R. 2012, MNRAS, 419, 479
Evans, N. J., II, Dunham, M. M., Jørgensen, J. K., et al. 2009, ApJS, 181, 321
Fioc, M., & Rocca-Volmerange, B. 1997, A&A, 326, 950
Fioc, M., & Rocca-Volmerange, B. 1999, arXiv:astro-ph/9912179
García-Vargas, M. L., Mollá, M., & Martín-Manjón, M. L. 2013, MNRAS, 432, 2746
Girardi, L., Bressan, A., Bertelli, G., & Chiosi, C. 2000, A&AS, 141, 371
Girardi, L., Bertelli, G., Bressan, A., et al. 2002, A&A, 391, 195
Girardi, L., Dalcanton, J., Williams, B., et al. 2008, PASP, 120, 583
Kang, Y., Bianchi, L., & Rey, S.-C. 2009, ApJ, 703, 614
Kennicutt, R. C., Jr. 1998, ARA&A, 36, 189
Kennicutt, R. C., & Evans, N. J. 2012, ARA&A, 50, 531
Kotulla, R., Fritze, U., Weilbacher, P., & Anders, P. 2009, MNRAS, 396, 462
Kurucz, R.L. 1991, in *Stellar Atmospheres, Beyond Classical Limits*, Crivellari L., Hubeny I., Hummer D.G. eds., Kluwer, Dordrecht, p. 441 (ATLAS9) `http//kurucz.harvard.edu/`
Johnson, B. D., Weisz, D. R., Dalcanton, J. J., et al. 2013, ApJ, 772, 8
Hao, C.-N., Kennicutt, R. C., Johnson, B. D., et al. 2011, ApJ, 741, 124
Hirashita, H., Buat, V., & Inoue, A. K. 2003, A&A, 410, 83
McKee, C. F., & Ostriker, E. C. 2007, ARA&A, 45, 565
Lada, C. J., Lombardi, M., Román-Zuñiga, C., Forbrich, J., & Alves, J. F. 2013, ApJ, 778, 133
Leitherer, C., Schaerer, D., Goldader, J. D., et al. 1999, ApJS, 123, 3
Leitherer, C., Ekström, S., Meynet, G., et al. 2014, ApJS, 212, 14
Lejeune, T., Cuisinier, F., & Buser, R. 1997, A&AS, 125, 229
Lejeune, T., Cuisinier, F., & Buser, R. 1998, A&AS, 130, 65
Leroy, A. K., Bigiel, F., de Blok, W. J. G., et al. 2012, AJ, 144, 3
Madau, P., & Dickinson, M. 2014, ARA&A, 52, 415
Maraston, C. 1998, MNRAS, 300, 872
Maraston, C. 2005, MNRAS, 362, 799
Marigo, P., & Girardi, L. 2007, A&A, 469, 239
Marigo, P., Girardi, L., Bressan, A., et al. 2008, A&A, 482, 883
Martín-Manjón, M. L., García-Vargas, M. L., Mollá, M., & Díaz, A. I. 2010, MNRAS, 403, 2012
Martins, F., & Palacios, A. 2013, A&A, 560, A16
Mas-Hesse, J. M., & Kunth, D. 1991, A&AS, 88, 399
Meynet, G., Maeder, A., Schaller, G., Schaerer, D., & Charbonnel, C. 1994, A&AS, 103, 97
Murphy, E. J., Condon, J. J., Schinnerer, E., et al. 2011, ApJ, 737, 67
Mollá, M., García-Vargas, M. L., & Bressan, A. 2009, MNRAS, 398, 451
Otí-Floranes, H., & Mas-Hesse, J. M. 2010, A&A, 511, A61
Paczyński, B. 1970, Acta Astron., 20, 47
Paczynski, B. 1975, ApJ, 202, 558
Percival, S. M., Salaris, M., Cassisi, S., & Pietrinferni, A. 2009, ApJ, 690, 427
Perret, V., Renaud, F., Epinat, B., et al. 2014, A&A, 562, A1
Pietrinferni, A., Cassisi, S., Salaris, M., & Castelli, F. 2004, ApJ, 612, 168
Pietrinferni, A., Cassisi, S., Salaris, M., & Castelli, F. 2006, ApJ, 642, 797
Pietrinferni, A., Cassisi, S., Salaris, M., Percival, S., & Ferguson, J. W. 2009, ApJ, 697, 275
Rauch, T. 2003, A&A, 403, 709
Román-Zúñiga, C. G., Ybarra, J. E., Megías, G. D., et al. 2015, AJ, 150, 80
Salaris, M., Cassisi, S., Pietrinferni, A., Kowalski, P. M., & Isern, J. 2010, ApJ, 716, 1241
Salpeter, E. E. 1955, ApJ, 121, 161
Schaerer, D., & de Koter, A. 1997, A&A, 322, 598
Schaller, G., Schaerer, D., Meynet, G., & Maeder, A. 1992, A&AS, 96, 269
Schmutz, W., Leitherer, C., & Gruenwald, R. 1992, PASP, 104, 1164
Shore, S. N. 2002, The Tapestry of Modern Astrophysics, by Steven N. Shore, pp. 888. ISBN 0-471-16816-5. Wiley-VCH, October 2002
Simones, J. E., Weisz, D. R., Skillman, E. D., et al. 2014, ApJ, 788, 12
Smith, L. J., Norris, R. P. F., & Crowther, P. A. 2002, MNRAS, 337, 1309
Tantalo, R., & Chiosi, C. 2004, MNRAS, 353, 917
Taylor, M. B. 2005, Astronomical Data Analysis Software and Systems XIV, 347, 29
Tinsley, B. M., & Gunn, J. E. 1976, ApJ, 203, 52
Tinsley, B. M. 1980, Fund. Cosmic Phys., 5, 287
Vassiliadis, E., & Wood, P. R. 1994, ApJS, 92, 125
Westera, P., Lejeune, T., Buser, R., Cuisinier, F., & Bruzual, G. 2002, A&A, 381, 524
Wilkins, S. M., Gonzalez-Perez, V., Lacey, C. G., & Baugh, C. M. 2012, MNRAS, 427, 1490